IOPscience iopscience.iop.org

Home Search Collections Journals About Contact us My IOPscience

Effects of boron addition on a-$Si_{90}Ge_{10}$:H films obtained by low frequency plasma enhanced chemical vapour deposition

This article has been downloaded from IOPscience. Please scroll down to see the full text article.

2005 J. Phys.: Condens. Matter 17 3975

(http://iopscience.iop.org/0953-8984/17/25/023)

View the table of contents for this issue, or go to the journal homepage for more

Download details:
IP Address: 129.252.86.83
The article was downloaded on 28/05/2010 at 05:11

Please note that terms and conditions apply.

INSTITUTE OF PHYSICS PUBLISHING JOURNAL OF PHYSICS: CONDENSED MATTER

J. Phys.: Condens. Matter **17** (2005) 3975–3983 doi:10.1088/0953-8984/17/25/023

Effects of boron addition on a-$Si_{90}Ge_{10}$:H films obtained by low frequency plasma enhanced chemical vapour deposition

Arllene M Pérez[1,2], Francisco J Renero[1], Carlos Zúñiga[1], Alfonso Torres[1] and César Santiago[3]

[1] Instituto Nacional de Astrofísica, Óptica y Electrónica (INAOE), Luis E Erro # 1, Santa María Tonantzintla, CP 72840, Puebla, Puebla, Mexico
[2] Universidad Popular Autónoma del Estado de Puebla (UPAEP), 21 Sur 1103 Colonia Santiago, CP 72160, Puebla, Puebla, Mexico
[3] Universidad Politécnica de Tulancingo, Prolongación Guerrero 808 Colonia Caltengo, CP 43626, Tulancingo, Hidalgo, Mexico

E-mail: arllene@inaoep.mx, AMPerez@upaep.mx, paco@inaoep.mx, czuniga@inaoep.mx, cde@inaoep.mx and cesar_mexico@hotmail.com

Received 7 March 2005, in final form 9 May 2005
Published 10 June 2005
Online at stacks.iop.org/JPhysCM/17/3975

Abstract
Optical, structural and electric properties of (a-$(Si_{90}Ge_{10})_{1-y}B_y$:H) thin film alloys, deposited by low frequency plasma enhanced chemical vapour deposition, are presented. The chemical bonding structure has been studied by IR spectroscopy, while the composition was investigated by Raman spectroscopy. A discussion about boron doping effects, in the composition and bonding of samples, is presented. Transport of carriers has been studied by measurement of the conductivity dependence on temperature, which increases from 10^{-3} to 10^{1} Ω^{-1} cm^{-1} when the boron content varies from 0 to 50%. Similarly, the activation energy is between 0.62 and 0.19 eV when the doping increases from 0 to 83%. The optical properties have been determined from the film's optical transmission, using Swanepoel's method. It is shown that the optical gap varies from 1.3 to 0.99 eV.

1. Introduction

Hydrogenated amorphous silicon-based binary alloys are widely used in the development of photovoltaic solar cells [1]. By alloying a-Si:H and Ge, it is possible to narrow the band gap, which improves the wavelength response [2–4], and this effect appears independent of the preparation method (RF sputtering, cathodic sputtering, DC glow discharge or RF discharge). Thus, amorphous silicon germanium hydrogenated alloys (a-$Si_{1-x}Ge_x$:H) have been obtained by different techniques; and their optical, structural and electrical properties have been reported [3–6].

 © 2005 IOP Publishing Ltd Printed in the UK

We present a study of optical, structural and electrical properties of boron doped amorphous silicon germanium films (a-$(Si_{90}Ge_{10})_{1-y}B_y$:H), deposited with low frequency discharge [7, 8] from a gas mixture of $SiH_4 + GeH_4 + B_2H_6$. We had already reported the electrical characterization of hydrogenated and fluorinated a-SiGe; it was shown that for a-SiGe:H, the electrical conductivity is two orders higher than that for a-SiGe:F, H. Furthermore, the optical gap for a-SiGe:H, F is around 0.2 eV higher than that for a-SiGe:H. By designing a Schottky diode, we dealt with a-$Si_{90}Ge_{10}$:H, which has an optical gap of 1.33 eV, and electrical conductivity at room temperature of the order of $10^{-6}\ \Omega^{-1}\ \mathrm{cm}^{-1}$, one order higher than those reported in the literature [3, 4]; however the electrical contacts are not ohmic. In order to improve the electrical properties of this alloy, and to obtain ohmic contacts, we have studied the effects of boron doping on a-$Si_{90}Ge_{10}$:H.

2. Experimental details

The samples of amorphous silicon germanium boron films were prepared by low frequency plasma enhanced chemical vapour deposition (LF PECVD), using an AMP 3300 PECVD system from Applied Materials. SiH_4, GeH_4 and B_2H_6 were the gas sources, and hydrogen the dilutor gas. The films were deposited at the substrate temperature $T_s = 300\,^{\circ}\mathrm{C}$. The parameters of deposition were the pressure ($P = 0.6$ Torr), power ($W = 350$ W) and frequency ($f = 110$ kHz). To probe repeatability, three identical processes were performed, with twenty samples treated in each process.

The germanium gas phase composition X_{Ge} is defined as the gas flow ratio

$$X_{\mathrm{Ge}} = \frac{[\mathrm{GeH_4}]}{[\mathrm{SiH_4}] + [\mathrm{GeH_4}]}, \tag{1}$$

and it was 10%.

The boron gas phase composition Y_B is defined as the gas flow ratio

$$Y_{\mathrm{B}} = \frac{[\mathrm{B_2H_6}]}{[\mathrm{SiH_4}] + [\mathrm{GeH_4}] + [\mathrm{B_2H_6}]}, \tag{2}$$

and it was varied from 0 to 83%. Secondary-ion mass spectroscopy (SIMS) was used to prove that the boron gas phase composition is similar to the boron film concentration.

The thickness of the films, d, was measured by a profilometer from Tencor Instruments, model 200; five measurements were taken and the average value was reported.

The infrared absorption spectra of the films were measured by a Bruker IR Fourier spectrometer, model V22. One sample of the same c-Si substrate wafer of $2 \times 2\ \mathrm{cm}^2$, was used as the reference sample in the IR measurements. The wavenumber k was varied from 350 to 4000 cm^{-1}, and ten measurements were taken at different times. Oxidation effects were discarded. An estimate of the total hydrogen content, C_H, was obtained from Cardona *et al* [9], and it is given by

$$C_{\mathrm{H}} = A \int \frac{\alpha(\omega)}{\omega}\, \mathrm{d}\omega, \tag{3}$$

where $\alpha(\omega)$ is the absorption coefficient of the film at frequency ω and A is the proportionality constant.

A micro-Raman study was done using a green laser, with emission at 514 nm, in a Jobin-Yvon Olympus BX 41 microscope and SPEX 500 M spectrophotometer. In these measurements, the samples from the IR study were used, and three Raman spectra were measured for each sample.

To carry out the electrical properties measurement, aluminium electrodes in the form of stripes with 2 mm inter-electrode distance were deposited by e-gun evaporation on Corning 1737 glass substrates of 6 cm $\times$ 2 cm.

Table 1. Film thickness and deposition rate in a-$(Si_{90}Ge_{10})_{1-y}B_y$:H films.

Y_B (%)	Measured thickness (μm)	Calculated thickness (μm)	V_d (Å s^{-1})
0	0.19 ± 0.01	0.186	1.58
10	0.21 ± 0.01	0.214	1.75
33	0.25 ± 0.01	0.251	2.08
44	0.29 ± 0.01	0.291	2.42
50	0.3 ± 0.01	0.295	2.5
83	0.32 ± 0.01	0.324	2.67

The conductivity $\sigma(T)$, which depends on the temperature, was measured in order to obtain the electrical parameters of the transport. The bias voltage was set at 10 V. The measurements were done under dark conditions in a vacuum chamber, and the temperature was varied from 300 to 500 K. Two measurements were taken at each point. The conductivity characteristics were calculated from experimental $\sigma(T)$ curves.

The UV to NIR transmission spectra of the films were measured by a double-beam spectrometer, Spectronic Unicam, model UV 300 (only two spectra were measured, because the results obtained were the same). The spectral range was taken from 400 to 1100 nm; and a Corning glass 1737 of 2 cm $\times$ 2 cm was used as the reference glass. Thus, we got the optical absorption edge, the refractive index n, the film thickness d and the optical gap E_g. We define the optical gap as E_{04}, i.e., the energy at which the optical absorption coefficient is equal to 10^4 cm^{-1} [10]. At maximum transmission, we get the position and order of the interference fringes in a non-absorbing region of the spectra. Then, we fit to a parabolic expression for n as a function of energy using an assumed approximate film thickness. The measured asymptotic transmission is used to scale the deduced value of n and to provide the correct film thickness, which is compared with that measured by the profilometer. These values were used in the calculation of the optical absorption coefficient α, using standard formulae [11].

3. Results and discussion

3.1. Growth rate

The growth rate V_d, of the a-$(Si_{90}Ge_{10})_{1-y}B_y$:H films was calculated by dividing the measured film thickness by the deposition time, and the results are listed in table 1. It can be seen from table 1 that, as boron is added into the gas mixture, the growth rate increases from 0.26 to 0.44 Å s^{-1}. Besides this, the growth rate also shows an almost monotonic increases as Y_B increases from 0 to 83%. This trend can be explained as follows. As we will see, the germanium in the solid phase increases too with Y_B. The binding energy of Ge–H is smaller than that of Si–H or B–H. So, it will be easier to break the Ge–H bond than to break the Si–H or B–H bond. The larger mass of the Ge atom and the greater weakness of the Ge–H bond will lead to a larger incident flux of active radicals. Similar arguments can be applied to measurements and calculated thicknesses (see table 1).

3.2. Infrared absorption spectra

The IR absorption spectra are shown in figure 1; they were taken after the samples were removed from the vacuum chamber and exposed to the atmosphere for 10, 30, 60, 120, 1440, 2880 and 4320 min. The spectra obtained when Y_B is different from zero were the same, and oxidation in the atmosphere was neglected.

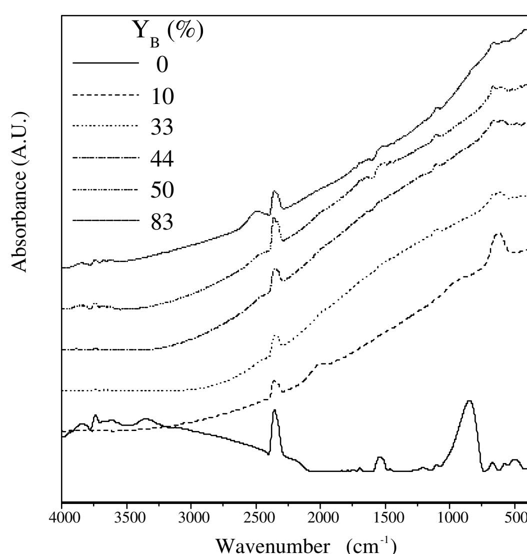

Figure 1. Absorption spectra of a-$(Si_{90}Ge_{10})_{1-y}B_y$:H films. (These spectra correspond to samples with 2880 min of atmospheric exposure.)

The peak, in the band $k = 630$–650 cm^{-1}, corresponds to the wagging mode of Ge–H and Si–H, and it appears for all samples [12]. When $Y_B = 0$, there is a peak at 845 cm^{-1}, which corresponds to the bending mode of $(SiH_2)_n$ [3]; and it disappears when Y_B increases. A weak peak at $k = 1200$ cm^{-1} appears for doped samples, which corresponds to B–B vibrations. At $k = 2300$ cm^{-1} a peak appears, corresponding to the stretching mode of Ge–H. When $Y_B = 10$ a peak appears at 2020 cm^{-1}; it corresponds to a B amorphous cluster (containing H). For the other samples this peak does not appear, but a similar peak centred at 1550 cm^{-1} is observed. A peak in the band $k = 2400$–2525 cm^{-1}, that is produced by the stretching mode of B–H [13], is observed when $Y_B \geqslant 33\%$.

In addition to the phenomena described above, we also observed a large and broad peak extending from 2750 to 3600 cm^{-1} when $Y_B = 0$. This is evidence that the film tends to oxidize in the atmosphere, a trend that increases with time.

Determination of hydrogen concentration by IR spectroscopy. The Si–H wagging mode was chosen for determining the hydrogen concentration; in this case $A = 1.6 \times 10^{19}$ cm^{-2} for Si and 1.1×10^{19} cm^{-2} for Ge [9].

The hydrogen concentration decreases from 2×10^{22} cm^{-3} to 1.5×10^{21} cm^{-3} when Y_B increases. This is due to the weaker bond strength of Ge–H compared with Si–H. This behaviour is associated with the increase in incorporation of Ge as Y_B increases.

3.3. Raman spectroscopy

Figure 2 shows the Raman spectra of a-$(Si_{90}Ge_{10})_{1-y}B_y$:H films, from which characteristic peaks can be seen. A main peak, located at 275 cm^{-1}, corresponds to the TO phonon of amorphous Ge. Another peak, at 380 cm^{-1}, corresponds to the LO phonon of a-Si (appearing for all samples). The peak centred at 470 cm^{-1} corresponds to the TO phonon of a-Si [14]. Peaks associated with B vibrations are not present. A preferential incorporation of Ge relative to the gas ratio is evident. If the full width at half-maximum (FWHM) of the TO peaks of

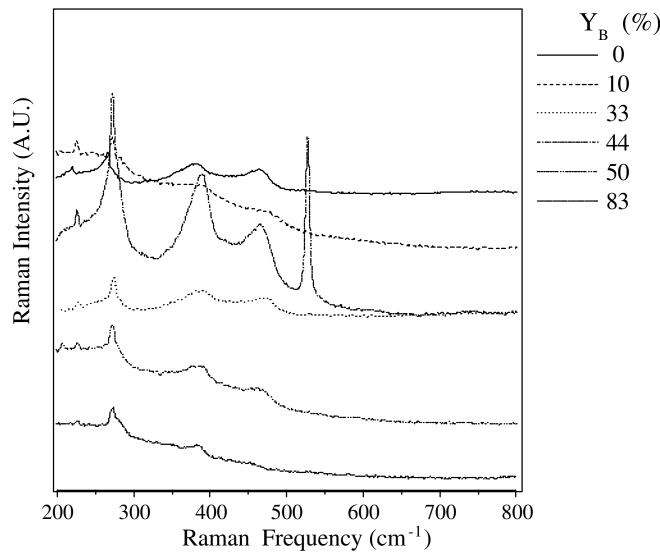

Figure 2. Raman spectra of a-$(Si_{90}Ge_{10})_{1-y}B_y$:H films.

Si is compared to that for Ge, it is found that the FWHM for a-Ge:H is smaller than that for a-Si:H, which implies better short range order, i.e., a smaller bond angle distribution of the Ge network compared with that for Si.

In a sample with 44% boron, a large peak is observed at 520 cm^{-1}, which is attributed to the local bending mode of Si–H [15].

3.4. Optical properties

Figure 3 shows a plot of the absorption coefficient versus the phonon energy. The spectra are deduced from optical transmission spectra using Tauc's method. The absorption spectrum of $Y_B = 50\%$ is almost the same as that of $Y_B = 44\%$; similar behaviours are observed when $Y_B = 33$ and 83%. The spectra are observed to shift smoothly to lower energies when Y_B increases. The oscillations observed in these spectra are caused by optical interference in the thin samples.

Figure 4 shows a plot of $(\alpha h\nu)^{1/2}$ versus photon energy, for the samples studied here. By extrapolating the linear part of the curve, the optical gap E_g, of the films can be extracted according to the empirical formula derived by Tauc [10]:

$$\sqrt{\alpha h\nu} = B(h\nu - E_g). \tag{4}$$

As figure 4 does not provide a good linear fit, an alternative method was used. It is a numerical simulation using a rigorous expression for the transmission [11], which is programmed in MatLab. The program calculates the optical gap using Tauc's model with an accuracy of 1%.

The optical gap values are listed in table 2. It can be seen from this table that the optical gap decreases from 1.33 to 0.99 eV when Y_B increases. Due to the higher concentration of germanium, especially that arising from the preferential incorporation of germanium, the optical gap will decrease more; when X_{Ge} is 10%, E_g approximately equal to 1.6 eV is expected but we obtained 1.33 eV.

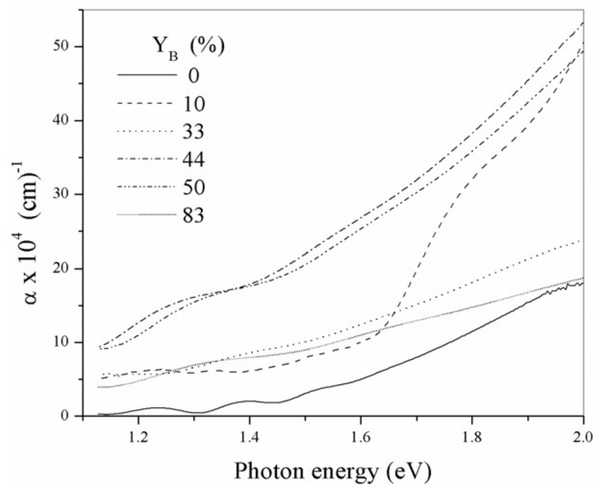

Figure 3. Absorption coefficient of a-$(Si_{90}Ge_{10})_{1-y}B_y$:H films.

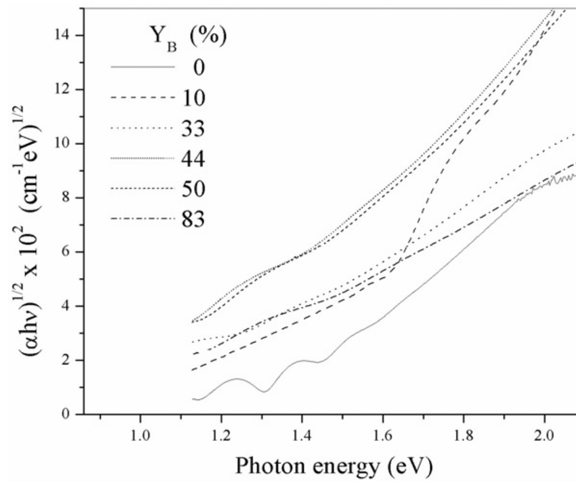

Figure 4. Tauc's plot for a-$(Si_{90}Ge_{10})_{1-y}B_y$:H films.

Table 2. Optical gaps in a-$(Si_{90}Ge_{10})_{1-y}B_y$:H films.

Y_B (%)	E_g (eV)
0	1.33
10	1.29
33	1.04
44	1.05
50	1.03
83	0.99

3.5. Electrical properties

Figure 5 shows a plot of the conductivity $\sigma(T)$ versus temperature. The parameters determined from these curves are listed in table 3. Electron conductivity in extended states is described

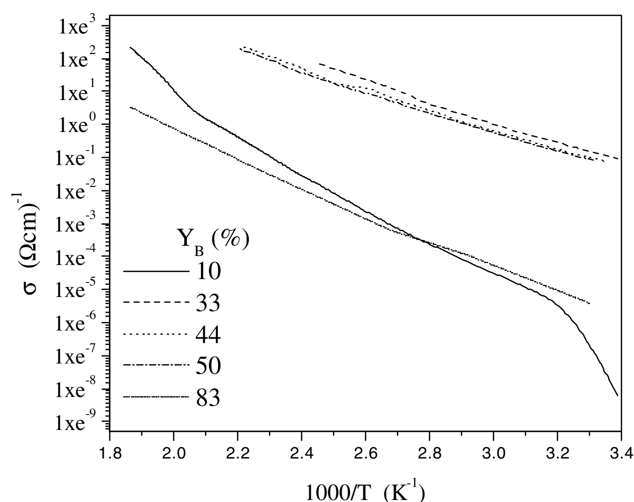

Figure 5. Temperature dependence of the conductivity of a-$(Si_{90}Ge_{10})_{1-y}B_y$:H films.

Table 3. Transport parameters of a-$(Si_{90}Ge_{10})_{1-y}B_y$:H films.

Y_B (%)	σ_0 (Ω^{-1} cm^{-1})	σ_{RT} (Ω^{-1} cm^{-1})	E_a (eV)	$\gamma \times 10^{-4}$ eV K^{-1}	E_F (eV)
0	3 400	10^{-6}	0.62	2.7	0.54
10	25 115	2.72×10^{-4}	0.26	4.2	0.13
33	23 491	0.354	0.26	4.1	0.14
44	16 541	0.333	0.25	3.8	0.14
50	11 647	0.337	0.24	3.5	0.13
83	1 885	4.5×10^{-3}	0.19	1.9	0.13

by [16]

$$\sigma(T) = \sigma_{min} e^{\gamma/k} \exp(-E_a/kT) = \sigma_0 \exp(-E_a/kT), \quad (5)$$

where σ_{min} is the minimal metallic conductivity ($\sigma_{min} = 200\ \Omega^{-1}\ \text{cm}^{-1}$ [17]), γ is the temperature coefficient (Fermi level), k is the Boltzmann constant, T is the temperature (in K), E_a is the activation energy and $\sigma_0 = \sigma_{min} e^{\gamma/k}$ is the pre-factor.

From figure 5, it can be seen that the conductivity of a-$(Si_{90}Ge_{10})$:H, at room temperature, is $\sigma_{RT} = 1.0 \times 10^{-6}\ \Omega^{-1}\ \text{cm}^{-1}$, and when Y_B is increased from 0 to 50%, the conductivity increases by five orders of magnitude. For high B content, the conductivity decreases.

After the boron content has increased by 50%, the conductivity saturates at around $\sigma = 0.3$ (Ω^{-1} cm^{-1}), and a decrease of the activation energy is observed (see table 3). The activation energy, E_a, is equal to the Fermi level at $T = 0$, and we observed significant changes of E_a as Y_B was varied. The Fermi level, E_F, moves from 0.54 to 0.13 eV when Y_B increases from 0 to 10%; then this value is conserved at higher Y_B.

Except for the undoped sample, the Meyer–Nelder rule holds for this material (see figure 6) [18].

4. Conclusions

In this paper, the structural, electrical and optical properties of a-$(Si_{90}Ge_{10})_{1-y}B_y$:H thin films deposited by the LF PECVD method using a SiH_4, GeH_4 and B_2H_6 mixture have been studied.

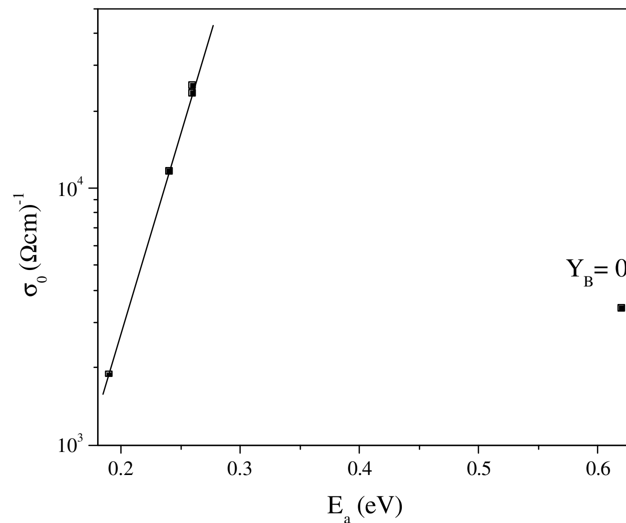

Figure 6. The Meyer–Nelder rule.

The phenomena observed can be summarized as follows:

(1) The film growth rate increases with incorporation of a relative small amount of B. There is not an exactly linear law.
(2) When the film is doped, any tendency to oxidize in the atmosphere disappears. This implies that the structure when Y_B is different from zero is less porous.
(3) The results suggest that the boron is incorporated in a-SiGe:H with a complex mix of bonds, but probably only a small percentage of the boron is electrically active.
(4) The optical gap varies with the B content, but preferential Ge incorporation in the solid phase is evident. This is demonstrated by Raman studies.
(5) The films with $Y_B = 33$, 44 and 50% demonstrated higher conductivity at room temperature than the others studied. The conductivity increases with the B content from 0 to 50%, and decreases for high B content.
(6) The activation energy decreases as the B content increases. The Fermi level varies when B is incorporated, but this value does not vary with Y_B.
(7) The Meyer–Nelder rule is observed for the film when it is doped.

Acknowledgments

The authors express their thanks to the technicians of the microelectronic laboratory of INAOE, to Dr Rosendo Lozada of BUAP and to CICATA-IPN Puebla.

References

[1] Shirahata K and Yukimoto Y 1982 *Amorphous Semiconductors Technologies and Devices* ed Y Hamakama (Amsterdam: North-Holland)
[2] Wickboldt P, Pang D, Paul W, Chen J, Zhong F, Cohen D and Williamson D 1997 *J. Appl. Phys.* **81-9** 6252–67
[3] Chou Y and Chen L 1998 *J. Appl. Phys.* **83-8** 4111–23
[4] Mackenzie K D, Egger J R, Leopold D J, Li Y M, Lin S and Paul W 1985 *Phys. Rev.* B **31-4** 2198–212

[5] Budaguan B G, Sherchenkov A A, Berdnikov A E, Metselaar J W and Aivazov A A 1999 *Mat. Res. Soc. Symp. Proc.* **557** 43–8
[6] Arllene M, Pérez G, Carlos Zuñiga I, Francisco J, Renero C and Alfonso Torres J 2005 *Opt. Eng.* **44** 04380
[7] Finger F and Beyer W 1998 *Properties of Amorphous Silicon and its Alloys* ed T Searle, London, chapter 1, pp 20–9
[8] Williams R F 1997 *Plasma Processing of Semiconductors* (London: Kluwer–Academic)
[9] Bermejo D and Cardona M 1979 *J. Non-Cryst. Solids* **32** 421–30
[10] Cody G D 1984 *Semiconductors and Semimetals, Part B Optical Properties* ed J I Pankove (New York: Academic) chapter 2, pp 11–82
[11] Swanepoel R 1983 *Rev. Sci. Instrum.* **16** 1214–22
[12] Perkowitz S 1993 *Optical Characterization of Semiconductors: Infrared, Raman and Photoluminescence Spectroscopy* (New York: Academic)
[13] Zanzucchi P J 1984 *Semiconductors and Semimetals Part B: Optical Properties* ed J I Pankove (New York: Academic) chapter 4, pp 113–40
[14] Minomura 1984 *Semiconductors and Semimetals Part A: Preparation and Structure* ed J I Pankove (New York: Academic) chapter 13, pp 273–90
[15] Lanin L S 1984 *Semiconductors and Semimetals Part B: Optical Properties* ed J I Pankove (New York: Academic) chapter 6, pp 159–98
[16] Elliot S R 1990 *Physics of Amorphous Materials* 2nd edn (New York: Longman Scientific Technical)
[17] Mott N F 1985 *J. Non-Cryst. Solids* **77/78** 115–20
[18] Beyer W and Overhof H 1984 *Semiconductors and Semimetals, Part C: Electronic and Transport Properties* ed J I Pankove (New York: Academic) chapter 8, pp 258–308